

Gluon saturation at RHIC and LHC

T. Lappi

Department of Physics, P.O. Box 35

40014 University of Jyväskylä, Finland

and

Helsinki Institute of Physics, P.O. Box 64

00014 University of Helsinki, Finland

Abstract

The physics of the initial conditions of heavy ion collisions is dominated by the nonlinear gluonic interactions of QCD. These lead to the concept of parton saturation. A consistent first-principles framework to understand this phenomenon is provided by the Color Glass Condensate (CGC). This talk reviews some aspects of the initial conditions at RHIC, and discusses implications for LHC heavy ion phenomenology. The CGC provides a way to compute bulk particle production and understand recent experimental observations of long range rapidity correlations in terms of the classical glasma field in the early stages of the collision. We discuss recent work showing that the multiplicity of gluons in the glasma follows a negative binomial distribution.

1 Introduction

The central rapidity region in high energy collisions originates from the interaction of the “slow” small x degrees of freedom, predominantly gluons, in the wavefunctions of the incoming hadrons or nuclei. At large energies these gluons form a dense system characterized by a *saturation scale* Q_s . The degrees of freedom with $p_T \lesssim Q_s$ are fully nonlinear Yang-Mills fields with large field strength $A_\mu \sim 1/g$ and occupation numbers $\sim 1/\alpha_s$; they can therefore be understood as classical fields radiated from the large x partons. Note that while this description is inherently nonperturbative, it is still based on a weak coupling argument, because the classical approximation requires $\alpha_s(Q_s)$ to be small and therefore $Q_s \gg \Lambda_{\text{QCD}}$. The Color Glass Condensate (CGC, for reviews see [1]) is a systematic effective theory (effective because the large x part of the wavefunction is integrated out) description of the classical small x degrees of freedom, and the term glasma [2] refers to the coherent, classical field configuration resulting from the collision of two such objects CGC.

A “pocket formula” [3] for estimating the energy and nuclear dependence of the saturation scale is $Q_s^2 \sim A^{1/3} x^{-0.3}$: nonlinear high gluon density effects are enhanced

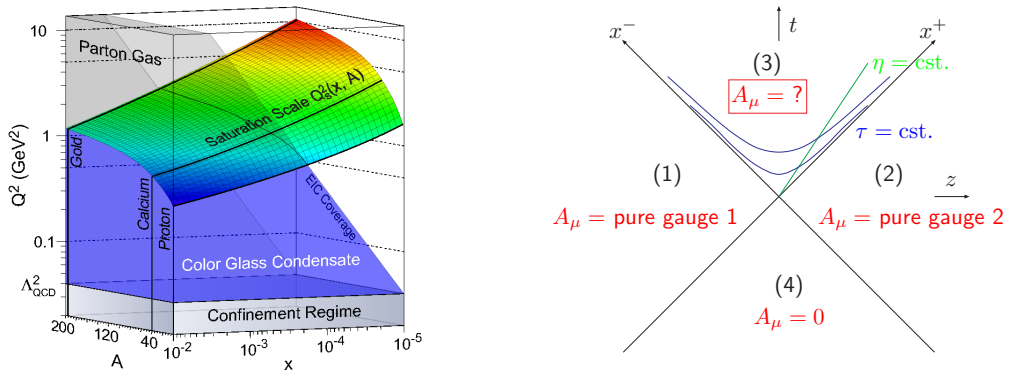


Figure 1: Left: Value of the saturation scale as a function of the momentum fraction and the atomic number. Right: Spacetime structure of the glasma fields. The field in regions (1) and (2) is a transverse pure gauge; the nontrivial glasma fields are present in region (3).

by going to small x and large nuclei. Ideally one would like to study the physics of the CGC at the Electron Ion Collider [4], but already based on fits to HERA data and simple nuclear geometry we have a relatively good idea of the magnitude of Q_s at RHIC energies as shown in Fig. 1 (left).

The focus of this talk is this dense field regime of the initial stage in a heavy ion collision. We shall first review some leading order classical field level results for gluon production at RHIC and the LHC. We shall then discuss a topic of more recent activity, computing fluctuations and correlations in the glasma.

2 Bulk gluon production

In order to compute particle production in the CGC framework one starts with the following setup [5]. The valence-like degrees of freedom of the two nuclei are represented by two classical color currents that are, because of their large longitudinal momenta (p^\pm) well localized on the light cone (in the variables conjugate to p^\pm , namely x^\mp): $J^\pm \sim \delta(x^\mp)$. These then generate the classical field that one wants to find. Working in light cone gauge (actually a temporal gauge $A_\tau = 0$ for the two nucleus problem), the field in the region of spacetime causally connected to only one of the nuclei is a transverse pure gauge, independently for each of the two nuclei. These pure gauge fields then give the initial condition on the future light cone ($\tau = \sqrt{2x^+x^-} = 0$) for the nontrivial gauge field after the collision. The spacetime structure of these fields is illustrated in Fig. 1 (right). The field inside the future light cone can then be computed either numerically [6] or analytically in different approximations (see e.g. [7] for recent work). The obtained result is then averaged over the configurations of the

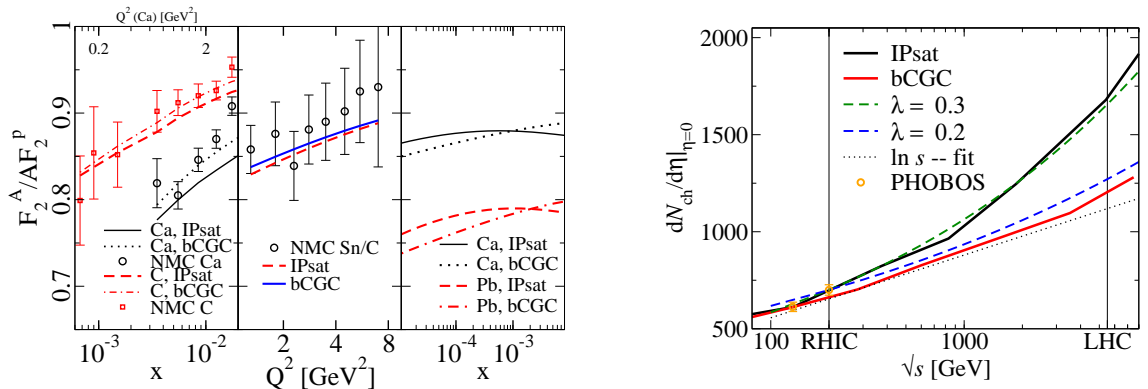


Figure 2: Left: Comparison of the fit [3] to existing nuclear DIS data from NMC. Right: Extrapolation of the gluon multiplicity to LHC energies, from [10]

sources J^μ with a distribution $W_y[J^\mu]$ that includes the nonperturbative knowledge of the large x degrees of freedom. The resulting fields can be decomposed into Fourier modes to get the gluon spectrum. This is the method that we will refer to as Classical Yang-Mills (CYM) calculations. Note that the average over configurations is a classical average over a probabilistic distribution. This is guaranteed by a theorem [8] ensuring the factorization of leading logarithmic corrections to gluon production into the quantum evolution of $W_y[J^\mu]$, analogously to the way leading logarithms of Q^2 are factorized into DGLAP-evolved parton distribution functions.

In the limit when either one or both of the color sources are dilute (the “pp” and “pA” cases), the CYM calculation can be done analytically and reduces to a convolution of unintegrated parton distributions that can include saturation effects. Although this approach (known as “KLN” after the authors of [9]) is not strictly valid for the collision of two dense systems, it has been widely used in the literature because it has the advantage of offering some analytical insight and making it easier to incorporate large- x ingredients into the calculation.

The CYM calculations [6] of gluon production paint a fairly consistent picture of gluon production at RHIC. The estimated value $Q_s \approx 1.2$ GeV from HERA data [3, 11] (corresponding to the MV model parameter $g^2\mu \approx 2.1$ GeV [12]) gives a good description of existing nuclear DIS data from the NMC collaboration, see Fig. 2 (left). The same value, when used in CYM calculations, leads to the estimate of $\frac{dN}{dy} \approx 1100$ gluons in the initial stage of a heavy ion collision. Assuming a rapid thermalization and nearly ideal hydrodynamical evolution this is consistent with the observed ~ 700 charged (~ 1100 total) particles produced in a unit of rapidity in central collisions. For other estimates of Q_s based on DIS data see Ref. [13].

The gluon multiplicity is, across different parametrizations, to a very good approximation proportional to $\pi R_A^2 Q_s^2/\alpha_s$. Thus the predictions for LHC collisions depend mostly on the energy dependence of Q_s . On this front there is perhaps more uncer-

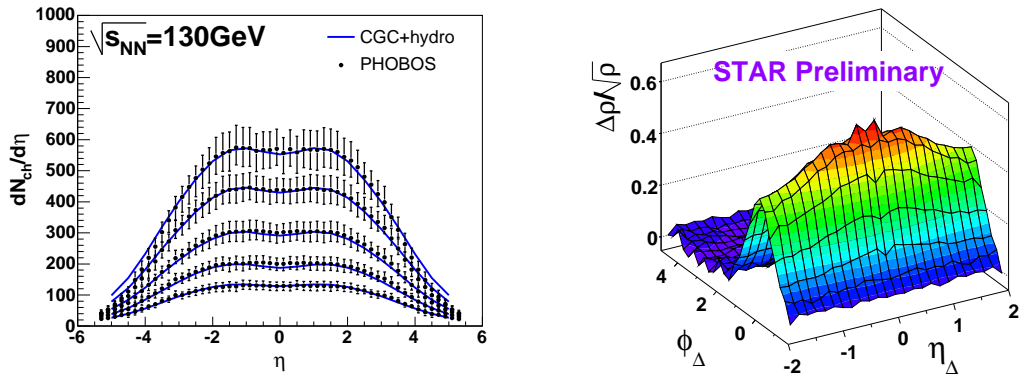


Figure 3: Left: rapidity dependence [18] Right: “Ridge” structure in the two particle correlation seen by STAR.

tainty than is generally acknowledged, since the estimates for $\lambda = d \ln Q_s^2 / d \ln 1/x$ vary between $\lambda = 0.29$ [14] and $\lambda = 0.18$ [15] in fixed coupling fits to HERA data, with a running coupling solution of the BK equation giving something in between these values [16]. This dominates the uncertainty in predictions for the LHC multiplicity, see Fig. 2 (right).

The RHIC collision energy is still too slow to clearly see any saturation effects in the rapidity dependence of the multiplicity around $y = 0$. A simple estimate for the effects of large x physics, such as momentum conservation, is to consider the typical $(1 - x)^4$ -dependence of gluon distributions at large x . Inserting $x = e^{\pm y} \langle p_{\perp} \rangle / \sqrt{s}$ leads to the estimate $\Delta y \sim \sqrt{8\sqrt{s} / \langle p_{\perp} \rangle}$ for the rapidity scale at which the large x effects contribute to the rapidity distribution around $y = 0$, with $\Delta y \sim 4$ RHIC and $\Delta y \sim 19$ at LHC. The large x contribution is an effect of order 1 at this scale, whereas small x evolution can be expected to give a much smaller effect [17] at a rapidity scale $\Delta y \sim 1/\alpha_s \sim 3$. Only at the LHC the large x effects will be mostly absent around midrapidity and one has a good possibility of seeing CGC effects in the rapidity dependence of the multiplicity. Figure 3 (left) shows a KLN-type calculation [18] of the rapidity dependence of the charged multiplicity at RHIC. The agreement is good, but it is practically insensitive to the rapidity dependence of the saturation scale from small x evolution [17]. A much more prominent signal that is present already at RHIC energies can be seen in two-particle correlations, Fig. 3 (right), that we shall turn to next.

3 Correlations

There are several signals in the RHIC data that point to strong correlations originating from the initial stage of the collision. One of these are the long range correlations

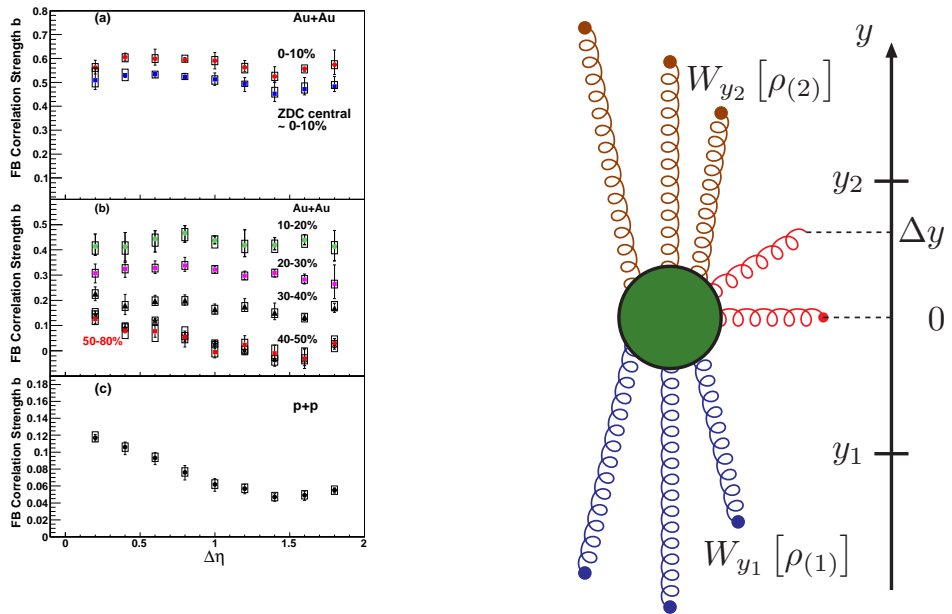


Figure 4: Left: STAR long range multiplicity correlation data from [19]. Right: Factorization of LLog corrections to gluon production: the phase space integral over Δy diverges and is cut off at the separation scales $y_{1,2}$. The dependence of the color charge density distributions $W_{y_{1,2}}$ on the cutoff cancels the leading logarithmic part of the dependence on $y_{1,2}$.

in the charged multiplicity reported by the STAR experiment [19] (see Fig. 4 left). The interpretation of this data is somewhat puzzling because of the interplay with the impact parameter induced, purely geometrical, correlations [20]. The observation that has gotten more attention recently is the “ridge” correlation, a structure that is more elongated in the η than the φ direction, see Fig. 3 (left) seen by several experiments [21]. Causality dictates that for very large rapidity separations these correlations were generated very early compared to the freezeout time, $\tau_{\text{corr}} \sim e^{-\Delta\eta/2}\tau_{\text{f.o.}}$. A separate question then is how early this time actually is at RHIC, see e.g. the discussion in Ref. [22].

The short range azimuthal correlation can be explained by a collimation effect of radial flow in the hydrodynamical evolution stage of the collision [23]. A natural explanation for the longitudinal structure of the ridge can be given in terms of boost invariant glasma [2] fields in the initial stages of the collision. The relevant two gluon correlation function in the glasma was computed (in the dilute large \mathbf{p}_T limit) in Ref. [24] and combined with a hydrodynamical computation to see the azimuthal structure in Ref. [25]. The calculation was generalized to a three gluon correlation in Ref. [26] and to arbitrary numbers of gluons in Ref. [27], showing

that the glasma naturally produces a negative binomial distribution for the gluon multiplicities, a “glittering” glasma. We shall first discuss some general aspects of computing multigluon correlations in the glasma before outlining the computation of the probability distribution at the end of this section.

The underlying physical reason for factorization is that this fluctuation with a large k^+ requires such a long interval in x^+ to be radiated that it must be produced well before and independently of the interaction with the other (left moving and thus localized in x^+) source. The concrete task is then to show that when one computes the NLO corrections to a given observable in the Glasma, all the leading logarithmic divergences can be absorbed into the RG evolution of the sources with the same Hamiltonian that was derived by considering only the DIS process. This is the proof of factorization in Refs. [8, 28, 29].

The leading logarithmic contribution comes from the longitudinal component of the integral over a momentum that is either the one of an additional produced gluon in the real term (see Fig. 4 right) or the loop momentum in the virtual contribution. It turns out that this LLog divergence can be expressed as the sum of two JIMWLK Hamiltonians acting on the expression for the leading order spectrum. This same Hamiltonian describes the RG evolution of the source distributions $W_y[\rho]$. It is most naturally expressed as

$$\mathcal{H} \equiv \frac{1}{2} \int d^2\mathbf{x}_T d^2\mathbf{y}_T D_a(\mathbf{x}_T) \eta^{ab}(\mathbf{x}_T, \mathbf{y}_T) D_b(\mathbf{y}_T) \quad (1)$$

in terms of Lie derivatives $D_a(\mathbf{x}_T)$ operating on the Wilson lines constructed from the source color charge densities. The kernel in Eq. (1) is a function of these same Wilson lines:

$$\eta^{ab}(\mathbf{x}_T, \mathbf{y}_T) = \frac{1}{\pi} \int d^2\mathbf{u}_T \frac{(\mathbf{x}_T - \mathbf{u}_T) \cdot (\mathbf{y}_T - \mathbf{u}_T)}{(\mathbf{x}_T - \mathbf{u}_T)^2 (\mathbf{y}_T - \mathbf{u}_T)^2} \left[U(\mathbf{x}_T) U^\dagger(\mathbf{y}_T) - U(\mathbf{x}_T) U^\dagger(\mathbf{u}_T) - U(\mathbf{u}_T) U^\dagger(\mathbf{y}_T) + 1 \right]^{ab}. \quad (2)$$

The fact that no other divergent terms appear is the proof of factorization; this is the central result of Ref. [8].

Let us then consider the probability distribution of the number of gluons produced in a small rapidity interval. It was shown in Ref. [28] that a similar factorization theorem holds for the leading logarithmic corrections to this probability distribution in the sense that we will briefly review here. It is convenient to define a generating functional

$$\mathcal{F}[z(\mathbf{p})] = \sum_{n=0}^{\infty} \frac{1}{n!} \int \left[\prod_{i=1}^n d^3\mathbf{p}_i (z(\mathbf{p}_i) - 1) \right] \frac{d^n N_n}{d^3\mathbf{p}_1 \cdots d^3\mathbf{p}_n}. \quad (3)$$

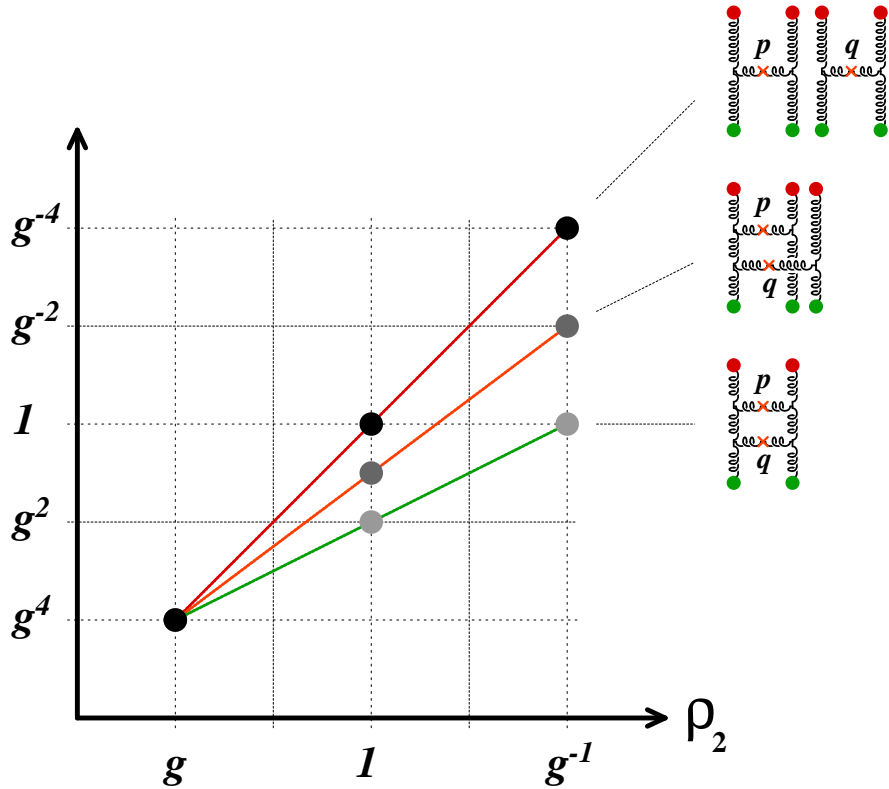


Figure 5: Relative importance of connected and disconnected diagrams to the two gluon correlation function. One of the color charge densities is considered large, $\rho_1 \sim 1/g$, whereas the other is allowed to vary between the “AA” case $\rho_2 \sim 1/g$ and the “pA” one $\rho_2 \sim g$. The order of the disconnected diagram, on top, is $g^4 \rho_1^4 \rho_2^4$, whereas the interference diagram in the middle is $g^4 \rho_1^3 \rho_2^3$ and the connected one, lowest, is $g^4 \rho_1^2 \rho_2^2$. In the “AA” case the disconnected diagram dominates, for the “pA” case all three are equally important. In the dilute “pp” limit only the connected diagram matters and both gluons are produced from the same BFKL ladder.

The Taylor coefficients of \mathcal{F} around $z = 1$ correspond to the moments of the probability distribution; integrated over the momenta of the produced gluons they are

$$\langle N \rangle \quad \langle N(N-1) \rangle \quad \dots \quad \langle N(N-1) \dots (N-n+1) \rangle. \quad (4)$$

The result of Ref. [28] is that when these moments are calculated to NLO accuracy, the leading logarithms can be resummed into the JIMWLK evolution of the sources completely analogously to the single inclusive gluon distribution. The resulting probability distribution can be written as:

$$\frac{d^n P_n}{d^3 \mathbf{p}_1 \dots d^3 \mathbf{p}_n} = \int_{\rho_1, \rho_2} W_Y[\rho_1] W_Y[\rho_2] \frac{1}{n!} \frac{dN}{d^3 \mathbf{p}_1} \dots \frac{dN}{d^3 \mathbf{p}_n} e^{-\int d^3 \mathbf{p} \frac{dN}{d^3 \mathbf{p}}}. \quad (5)$$

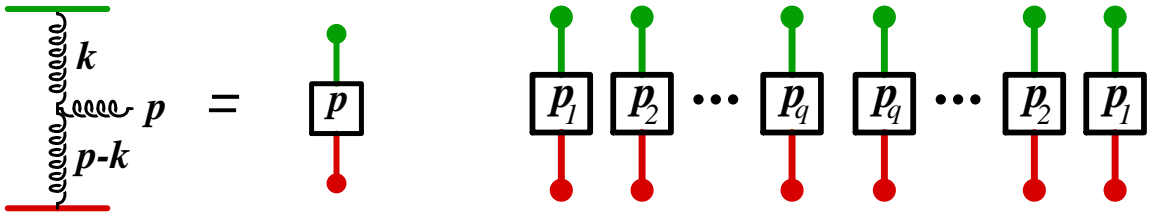


Figure 6: Left: Building block, Lipatov vertex coupled to two sources. Right: combinatorics of the sources. The combinatorial problem is to connect the dots on the upper and lower side (left- and right moving sources) pairwise.

Note that the Poissonian-looking form of the result is to some extent an artifact of our choosing to develop and truncate precisely the moments Eq. (3) that are simply $\langle N \rangle^n$ for a Poissonian distribution. Since in our power counting $N \sim 1/\alpha_s$, any contributions that would make the distribution Eq. (5) deviate from the functional form are of higher order in the weak coupling expansion of the moments (3) and are neglected in our calculation unless they are enhanced by large logarithms of x . Nevertheless it should be emphasized that in spite of appearances of Eq. (5) the probability distribution is in fact not Poissonian. To understand the nontrivial nature of this result it must be remembered that the individual factors of $\frac{dN}{d^3p_i}$ in Eq. (5) are all functionals of the *same* color charge densities $\rho_{1,2}$; thus the averaging over the ρ 's induces a correlation between them. These correlations are precisely the leading logarithmic modifications to the probability distribution; they have been resummed into the distributions W_y ; the functional form of the multigluon correlation function *under* the functional integral in Eq. (5) is the same as at leading order. This is the result of the proof in Ref. [28].

The calculation of multigluon correlation is in fact simplified in the strong field limit, where the leading contribution to particle production corresponds to the classical field and the correlations are encoded in the evolution of the sources [30]. In the “pA” case where one of the sources is assumed to be dilute, the situation becomes much more complicated, because the disconnected classical contributions are not the only dominant ones any more. This structure is illustrated in Fig. 5. A generalization of the formulation [31] to large rapidity separations between the produced gluons, as in the case of the “ridge” correlation is relatively straightforward but would take us too far here; we refer the reader to Ref. [31].

4 Glittering glasma

We can then apply this formalism to the calculation of the probability distribution of the number of gluons in the glasma [27]. We shall assume the “AA” power counting

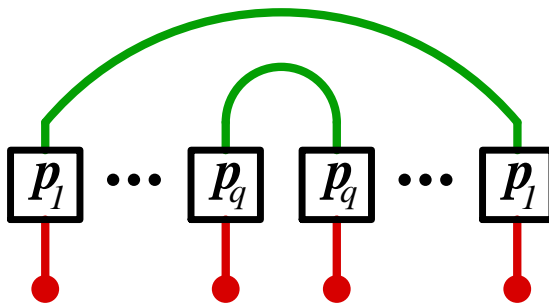


Figure 7: Dominant contributions are “rainbow” diagrams, where on one side (left- or rightmoving sources) the same sources in the amplitude and the complex conjugate are connected to each other.

of sources that are parametrically strong in g , but nevertheless work to the lowest nontrivial order in the color sources. Formally this would correspond to a power counting $\rho \sim g^{\epsilon-1}$ with a small $\epsilon > 0$. In this limit, as we have discussed, the dominant contributions to multiparticle correlations come from diagrams that are disconnected for fixed sources and become connected only after averaging over the color charge configurations. In other words, the dominant correlations are those arising from resummed large logarithms of the collision energy and are present already in the initial wavefunctions of the colliding nuclei.

Working with the MV model Gaussian probability distribution

$$W[\rho] = \exp \left[- \int d^2 \mathbf{x}_T \frac{\rho^a(\mathbf{x}_T) \rho^a(\mathbf{x}_T)}{g^4 \mu^2} \right] \quad (6)$$

computing the correlations in the linearized approximation is a simple combinatorial problem. Each gluon is produced from two Lipatov vertices (see Fig. 6 left), one in the amplitude and the other in the complex conjugate. The combinatorial factor is obtained by counting the different ways of contracting the sources pairwise (see Fig. 6 right). The dominant contributions are “rainbow” diagrams, Fig. 7, where on the side of one of the sources a line with momentum \mathbf{p}_T in the amplitude is connected to a line with the same momentum in the complex conjugate amplitude. These are the contributions containing a maximally infrared divergent integral in the momentum circulating in the lower (“non-rainbow”) side of the diagram. This divergence is then regulated by the transverse correlation scale of the problem, Q_s . When integrated over the momenta of the produced gluons one obtains the factorial moments of the multiplicity, which define the whole probability distribution. It can be expressed in terms of two parameters, the mean multiplicity \bar{n} , and a parameter k describing the width of the distribution. The result of the combinatorial exercise is that the number of contributing diagrams, each with an equal contribution, is $2^q (q-1)!$. The factorial

moments $m_q \equiv \langle N^q \rangle - \text{disc.}$ are

$$m_q = (q-1)! k \left(\frac{\bar{n}}{k} \right)^q \text{ with parameters} \quad (7)$$

$$k \approx \frac{(N_c^2 - 1) Q_s^2 S_\perp}{2\pi} \quad (8)$$

$$\bar{n} = f_N \frac{1}{\alpha_s} Q_s^2 S_\perp. \quad (9)$$

These moments define a *negative binomial* distribution with parameters k and \bar{n} , which has been used as a phenomenological observation in high energy hadron and nuclear collisions already for a long time [32]. In terms of the glasma flux tube picture this result has a natural interpretation. The transverse area of a typical flux tube is $1/Q_s^2$, and thus there are $Q_s^2 S_\perp = N_{\text{FT}}$ independent ones. Each of these radiates particles independently into $N_c^2 - 1$ color states in a Bose-Einstein distribution (see e.g. [33]). A sum of $k \approx N_{\text{FT}}(N_c^2 - 1)$ independent Bose-Einstein-distributions is precisely equivalent to a negative binomial distribution with parameter k .

Acknowledgements Numerous conversations with F. Gelis, L. McLerran and R. Venugopalan are gratefully acknowledged. The author is supported by the Academy of Finland, contract 126604.

References

- [1] E. Iancu and R. Venugopalan, The color glass condensate and high energy scattering in QCD, in *Quark gluon plasma*, edited by R. Hwa and X. N. Wang, World Scientific, 2003, arXiv:hep-ph/0303204; H. Weigert, Prog. Part. Nucl. Phys. **55**, 461 (2005), [arXiv:hep-ph/0501087].
- [2] T. Lappi and L. McLerran, Nucl. Phys. **A772**, 200 (2006), [arXiv:hep-ph/0602189].
- [3] H. Kowalski, T. Lappi and R. Venugopalan, Phys. Rev. Lett. **100**, 022303 (2008), [arXiv:0705.3047 [hep-ph]].
- [4] A. Deshpande, R. Milner, R. Venugopalan and W. Vogelsang, Ann. Rev. Nucl. Part. Sci. **55**, 165 (2005), [arXiv:hep-ph/0506148].
- [5] A. Kovner, L. D. McLerran and H. Weigert, Phys. Rev. **D52**, 3809 (1995), [arXiv:hep-ph/9505320].

- [6] A. Krasnitz, Y. Nara and R. Venugopalan, Phys. Rev. Lett. **87**, 192302 (2001), [arXiv:hep-ph/0108092]; T. Lappi, Phys. Rev. **C67**, 054903 (2003), [arXiv:hep-ph/0303076]; A. Krasnitz, Y. Nara and R. Venugopalan, Nucl. Phys. **A727**, 427 (2003), [arXiv:hep-ph/0305112].
- [7] J.-P. Blaizot and Y. Mehtar-Tani, Nucl. Phys. **A818**, 97 (2009), [arXiv:0806.1422 [hep-ph]].
- [8] F. Gelis, T. Lappi and R. Venugopalan, Phys. Rev. **D78**, 054019 (2008), [arXiv:0804.2630 [hep-ph]].
- [9] D. Kharzeev and M. Nardi, Phys. Lett. **B507**, 121 (2001), [arXiv:nucl-th/0012025]; D. Kharzeev and E. Levin, Phys. Lett. **B523**, 79 (2001), [arXiv:nucl-th/0108006].
- [10] T. Lappi, J. Phys. **G35**, 104052 (2008), [arXiv:0804.2338 [hep-ph]].
- [11] H. Kowalski and D. Teaney, Phys. Rev. **D68**, 114005 (2003), [arXiv:hep-ph/0304189].
- [12] T. Lappi, Eur. Phys. J. **C55**, 285 (2008), [arXiv:0711.3039 [hep-ph]].
- [13] A. Freund, K. Rummukainen, H. Weigert and A. Schafer, Phys. Rev. Lett. **90**, 222002 (2003), [arXiv:hep-ph/0210139]; N. Armesto, C. A. Salgado and U. A. Wiedemann, Phys. Rev. Lett. **94**, 022002 (2005), [arXiv:hep-ph/0407018].
- [14] K. J. Golec-Biernat and M. Wusthoff, Phys. Rev. **D59**, 014017 (1999), [arXiv:hep-ph/9807513].
- [15] H. Kowalski, L. Motyka and G. Watt, Phys. Rev. **D74**, 074016 (2006), [arXiv:hep-ph/0606272].
- [16] J. L. Albacete, Phys. Rev. Lett. **99**, 262301 (2007), [arXiv:0707.2545 [hep-ph]].
- [17] T. Lappi, Phys. Rev. **C70**, 054905 (2004), [arXiv:hep-ph/0409328].
- [18] T. Hirano and Y. Nara, Nucl. Phys. **A743**, 305 (2004), [arXiv:nucl-th/0404039].
- [19] STAR, B. I. Abelev *et al.*, arXiv:0905.0237 [nucl-ex].
- [20] T. Lappi and L. McLerran, arXiv:0909.0428 [hep-ph].
- [21] J. Putschke, J. Phys. **G34**, S679 (2007), [arXiv:nucl-ex/0701074]; STAR, M. Daugherty, J. Phys. **G35**, 104090 (2008), [arXiv:0806.2121 [nucl-ex]]; PHOBOS, B. Alver *et al.*, J. Phys. **G35**, 104080 (2008), [arXiv:0804.3038 [nucl-ex]].

- [22] J. L. Nagle, arXiv:0907.2707 [nucl-ex].
- [23] S. A. Voloshin, Phys. Lett. **B632**, 490 (2006), [arXiv:nucl-th/0312065]; E. V. Shuryak, Phys. Rev. **C76**, 047901 (2007), [arXiv:0706.3531 [nucl-th]]; C. A. Pruneau, S. Gavin and S. A. Voloshin, Nucl. Phys. **A802**, 107 (2008), [arXiv:0711.1991 [nucl-ex]].
- [24] A. Dumitru, F. Gelis, L. McLerran and R. Venugopalan, Nucl. Phys. **A810**, 91 (2008), [arXiv:0804.3858 [hep-ph]].
- [25] S. Gavin, L. McLerran and G. Moschelli, Phys. Rev. **C79**, 051902 (2009), [arXiv:0806.4718 [nucl-th]].
- [26] K. Dusling, D. Fernandez-Fraile and R. Venugopalan, Nucl. Phys. **A828**, 161 (2009), [arXiv:0902.4435 [nucl-th]].
- [27] F. Gelis, T. Lappi and L. McLerran, Nucl. Phys. **A828**, 149 (2009), [arXiv:0905.3234 [hep-ph]].
- [28] F. Gelis, T. Lappi and R. Venugopalan, Phys. Rev. **D78**, 054020 (2008), [arXiv:0807.1306 [hep-ph]].
- [29] F. Gelis, T. Lappi and R. Venugopalan, Int. J. Mod. Phys. **E16**, 2595 (2007), [arXiv:0708.0047 [hep-ph]].
- [30] D. Kharzeev, E. Levin and L. McLerran, Nucl. Phys. **A748**, 627 (2005), [arXiv:hep-ph/0403271]; N. Armesto, L. McLerran and C. Pajares, Nucl. Phys. **A781**, 201 (2007), [arXiv:hep-ph/0607345].
- [31] F. Gelis, T. Lappi and R. Venugopalan, Phys. Rev. **D79**, 094017 (2008), [arXiv:0810.4829 [hep-ph]]; T. Lappi, Acta Phys. Polon. **B40**, 1997 (2009), [arXiv:0904.1670 [hep-ph]].
- [32] UA1, G. Arnison *et al.*, Phys. Lett. **B123**, 108 (1983); UA5, G. J. Alner *et al.*, Phys. Lett. **B160**, 193 (1985); UA5, G. J. Alner *et al.*, Phys. Lett. **B160**, 199 (1985); UA5, R. E. Ansorge *et al.*, Z. Phys. **C37**, 191 (1988); PHENIX, S. S. Adler *et al.*, Phys. Rev. **C76**, 034903 (2007), [arXiv:0704.2894 [nucl-ex]]; PHENIX, A. Adare *et al.*, Phys. Rev. **C78**, 044902 (2008), [arXiv:0805.1521 [nucl-ex]].
- [33] K. Fukushima, F. Gelis and T. Lappi, arXiv:0907.4793 [hep-ph].